

**United States
Department of
Agriculture**

**Natural Resources
Conservation
Service**

**11 Campus Boulevard,
Suite 200
Newtown Square, PA 19073**

Subject: SOI – Geophysical Field Assistance

Date: 17 December 2008

To: Dr. Henry Lin
Assistant Professor of Hydropedology/Soil Hydrology
Crop & Soil Sciences Department
415 Agricultural Sciences and Industries Building
Pennsylvania State University
University Park, PA 16802

Edgar White
State Soil Scientist
USDA-NRCS
One Credit Union Place, Suite 340
Harrisburg, PA 17110-2993

Purpose:

Two separate visits were made to Pennsylvania State University to assist Dr Henry Lin and his graduate students complete hydrogeological investigations using geophysical methods. Multiple, ground-penetrating radar (GPR) surveys were conducted across three small grid located within the Shale Hills Catchment (Huntingdon County) to further evaluate GPR processing and imaging software programs, and the effectiveness of GPR for detecting the infiltration of water in natural settings. The integration of global positioning systems (GPS) with GPR to map bedrock depths within Shale Hills Catchment was also explored. In addition, a high-intensity electromagnetic induction (EMI) survey was completed at Pennsylvania State University's Klepler Farm in Centre County.

Activities:

Field activities were completed on 20 October and during the period of 10 to 12 November 2008.

Participants:

Jim Doolittle, Research Soil Scientist, USDA-NRCS-NSSC, Newtown Square, PA
Henry Lin, Assistant Professor of Hydropedology/Soil Hydrology, Department of Crop & Soil Sciences, PSU, University Park, PA
Jun Zhang, PhD Student, Department of Crop & Soil Sciences, PSU, University Park, PA
Quing Zhu, PhD Student, Department of Crop & Soil Sciences, PSU, University Park, PA
Kenneth Takagi, Graduate Student, Department of Crop & Soil Sciences, PSU, University Park, PA

Summary:

1. Water infiltration studies at Shale Hills have drawn attention to the inherent difficulty in repeating detailed GPR grid surveys under natural terrain conditions. These surveys are challenged by the precise placement of recording antenna positions and variations in the rate of data acquisition along traverse lines.
2. At the small, permanent, detailed grid, located on the lower portion of a swale, two GPR surveys were completed using a 400 MHz antenna. A time-lapsed comparison of GPR imagery showed noticeable differences in subsurface reflections amplitudes between the two collection events. Differences in reflected signal amplitudes are largely attributed to differences in the number of gain break points and gain settings used for the two surveys. Disregarding differences in reflected signal amplitudes, subsurface spatial patterns were remarkably similar on prepared 3D pseudo-images, which were compiled from data collected a month apart. It is recommended that an additional survey of the site be conducted under moister conditions (March) with the same gain settings and number of break points as used in the November 2008 survey.
3. Two infiltration experiments were completed in the Shale Hills Catchment with a 400 MHz antenna; one in an area of Weikert soils and one in an area of Rushtown soils. These detailed studies provided baseline information, revealed limitations of field methods used, and helped to improve survey protocol for investigations conducted in forested environment.
4. In my near thirty years of work with GPR, I have never before conducted detailed, time-lapsed surveys of gridded area. Unfortunately, errors, missteps, and oversights have occurred. Experiences gained from these studies will undoubtedly lead to more practical and effective protocol for similar applications of ground-penetrating radar. Following the reported field

work, I have talked with the staff of GSSI to remedy or at least minimize these problems, and to improve the processing, visualization, and interpretation of collected data. Their suggestions have been included in this report.

It was my pleasure to participate in these studies and to work with the graduate students at Pennsylvania State University.

With kind regards,

James A. Doolittle
Research Soil Scientist
Soil Survey Research Staff
National Soil Survey Center

cc:

- B. Ahrens, Director, National Soil Survey Center, USDA-NRCS, Federal Building, Room 152, 100 Centennial Mall North, Lincoln, NE 68508-3866
- S. Carpenter, MLRA Office Leader, USDA-NRCS, 75 High Street, Room 301, Morgantown, WV 26505
- M. Golden, Director, Soil Survey Division, USDA-NRCS, Room 4250 South Building, 14th & Independence Ave. SW, Washington, DC 20250
- W. Tuttle, Soil Scientist (Geophysical), National Soil Survey Center, USDA-NRCS, P.O. Box 60, 207 West Main Street, Rm. G-08, Federal Building, Wilkesboro, NC 28697
- L. West, National Leader, Soil Survey Research and Laboratory Staff, National Soil Survey Center, USDA-NRCS, Federal Building, Room 152, 100 Centennial Mall North, Lincoln, NE 68508-3866

Background:

Robinson et al. (2008) discusses the use of near surface geophysical methods, principally electrical and magnetic methods, to measure geologic structure and identify flow paths in watersheds and catchments, which are defined at different spatial scales. These researchers briefly discuss the use of ground-penetrating radar (GPR) to capture the movement of water through the subsurface under control experiments, but provide no examples. The present studies are directed towards a better understanding of hydrogeologic properties within Shale Hills Catchment, Huntingdon County, Pennsylvania. As a part of these studies, the practical and effective use of GPR is being explored. As these are ground-breaking and innovative studies, the development of appropriate field protocol is being explored. In these studies, GPR is being used to profile the bedrock topography, characterize lithologic and stratigraphic layers which influence the flow of ground waters.

On radar records, temporal variations in signal amplitudes and time shifts in the position of subsurface reflectors are attributed to differences soil moisture contents. The *relative dielectric permittivity* (E_r) of soil materials is largely a function of their moisture contents. As a consequence, the amount of energy reflected back from a subsurface interface is contingent upon the abruptness and difference in moisture contents between two soil layers. The more abrupt and contrasting the difference in moisture contents between two adjoining layers, the higher the amplitudes of the reflected signals. Conyers (2004) observed changes in the relative amplitudes of reflected radar signals from the same site and features under different soil moisture conditions (e.g., dry versus wet). He concluded that, depending on soil type, many subsurface features are visible only under certain moisture conditions, which will vary both spatially and temporally.

The greater and more abrupt the contrast in electromagnetic properties between two subsurface layers, the greater the amount of energy reflected back to the antenna, and the more intense and conspicuous will be the amplitude of reflected signals on the radar record. The *reflection coefficient*, R , is a measure of the differences in dielectric properties that exist between two adjoining layers or materials. The reflection coefficient is proportional to reflection strength and is expressed as (after Daniels, 2004):

$$R = \frac{\sqrt{E_{r2}} - \sqrt{E_{r1}}}{\sqrt{E_{r2}} + \sqrt{E_{r1}}} \quad [1]$$

where E_{r1} and E_{r2} are the relative dielectric permittivity of adjoining materials 1 and 2. As evident in equation [1], R is dependent on the difference in the E_r that exists between the two adjoining layers or materials. The reflection coefficient will have a positive value, when $E_{r2} > E_{r1}$, and a negative value, when $E_{r2} < E_{r1}$. These differences will affect the pulse waveform and change the phase of the reflected pulse. On radar records, these differences will be manifested as different phase patterns (Daniels, 2004).

With increasing soil moisture contents, the E_r of soils will increase resulting in greater signal loss, lower propagation velocities, and increased travel time to subsurface interfaces. On radar records, increased soil moisture contents will result in time shifts with reflectors appearing at later recording times.

This report briefly summarizes some of the findings from recent GPR surveys that were completed in Shale Hills Catchment. Jun Zhang, as part of his research project, is more fully evaluating the collected two-dimensional (2D) radar records and three-dimensional (3D) pseudo-images using advance processing and visualization techniques.

Equipment:

The radar unit is the TerraSIRch Subsurface Interface Radar (SIR) System-3000 (SIR-3000), manufactured by Geophysical Survey Systems, Inc. (GSSI; Salem, NH).¹ The SIR-3000 consists of a digital control unit (DC-3000) with keypad, SVGA video screen, and connector panel. A 10.8-volt lithium-ion rechargeable battery powers the system. The SIR-3000 weighs about 9 lbs (4.1 kg) and is backpack portable. An antenna with a center frequency of 400 MHz was used in the reported studies. With an antenna, the SIR-3000 requires two people to operate. Daniels (2004) discusses the use and operation of GPR.

The RADAN for Windows (version 6.6) software program (GSSI) was used to process the radar records shown in this report.¹ Processing included: header editing, setting the initial pulse to time zero, color table and transformation selection, range gain adjustments, signal stacking, migration, and high-pass filtration (see Daniels (2004) for a discussion of these techniques). The Super 3D QuickDraw program developed by GSSI was used to construct 3D pseudo-images of radar records collected at the grid sites. In an attempt to show differences in reflected signal amplitudes that are associated with changes in relative soil moisture contents, a Hilbert transformation was used on some data sets. The Hilbert transformation reconstructs the reflected signal, indicates subtle differences in relative signal magnitudes, and displays associated spatial patterns.

¹ Manufacturer's names are provided for specific information; use does not constitute endorsement.

The EM38DD meter, manufactured by Geonics limited (Mississauga, Ontario) was used in a high-intensity survey at Klepler Farm.² This meter requires only one person to operate. No ground contact is required with this instrument. The EM38DD meter consists of two, coupled EM38 meters. Each EM38 meter weighs about 3 kg (6.6 lbs), has a 1-m intercoil spacing, and operates at a frequency of 14,600 Hz. When placed on the soil surface, these meters provide nominal penetration depths of about 0.75 m (meter positioned in the horizontal dipole orientation) and 1.5 m (meter positioned in the vertical dipole orientation). Operating procedures for the EM38DD meter are described by Geonics Limited (2000).

To complete the high-intensity EMI survey at Klepler Farm, the EM38DD was operated in the continuous mode. The meter was placed in a plastic sled and towed behind an all-terrain vehicle (ATV). An Allegro CX field computer (Juniper Systems, North Logan, UT) was used to record and store both EMI and position data². The coordinates of each EC_a measurement were recorded with a Trimble AgGPS114 L-band DGPS (differential GPS) antenna (Trimble, Sunnyvale, CA).² The Trackmaker38DD software program developed by Geomar Software Inc. (Mississauga, Ontario) was used to record, store, and process EC_a and GPS data.²

Ground-Penetrating Radar Surveys:

Calibration of GPR:

Ground-penetrating radar is a time scaled system. The system measures the time that it takes electromagnetic energy to travel from an antenna to an interface (e.g., bedrock, soil horizon, stratigraphic layer) and back. To convert the travel time into a depth scale, either the velocity of pulse propagation or the depth to a reflector must be known. The relationships among depth (D), two-way pulse travel time (T), and velocity of propagation (v) are described in equation [1] (after Daniels, 2004):

$$v = 2D/T \quad [1]$$

The velocity of propagation is principally affected by the relative dielectric permittivity (E_r) of the profiled material(s) according to equation [2] (after Daniels, 2004):

$$E_r = (C/v)^2 \quad [2]$$

Where C is the velocity of propagation in a vacuum (0.298 m/ns). Velocity is expressed in meters per nanosecond (ns). In soils, the amount and physical state (temperature dependent) of water have the greatest effect on the E_r and v. At the time of these studies, soils were relatively dry.

Based on the measured depth and the two-way pulse travel time to a known subsurface reflector (metal plate buried at 50 cm), the velocity of propagation and the relative dielectric permittivity through the upper part of soil profiles were estimated using equations [1] and [2]. In an area of Rushtown soils, the estimated E_r for the October and November GPR surveys were 8.05 and 7.42, respectively. These permittivities resulted in a v 0.1050 and 0.1094 m/ns for the October and November surveys, respectively.

Field Methods:

GPR-GPS Study:

The SIR-3000 system provides a setup for the use of a GPS receiver with a serial data recorder (SDR) and a GPS receiver. With this setup, each scan on radar records can be georeferenced (position/time matched). Following data collection, a subprogram within the RADAN for Windows (version 6.6) software is used to proportionally adjust the position of each radar scan according to the time stamp of the two nearest positions recorded with the GPS receiver. In this study, a Trimble AG114 GPS receiver was used to collect position data at a rate of one measurement/sec.

Table 1. Taxonomic classifications of the soils scanned with GPR within the Shale Hills Catchment.

SOIL SERIES	TAXONOMIC CLASSIFICATION
Berks	Loamy-skeletal, mixed, active, mesic Typic Dystrudepts
Rushtown	Loamy-skeletal over fragmental, mixed, active, mesic Typic Dystrudepts
Weikert	Loamy-skeletal, mixed, active, mesic Lithic Dystrudepts

Five radar traverses were completed across a portion of the south-facing summit and back slope components of the Shale Hills Catchment. This area of the catchment afforded the greatest possibility for acceptable satellite reception. The arrangement of this narrow, steeply sloping, forested catchment was extremely unfavorable for good satellite reception. With the SIR-3000 system, use of

² Manufacturer's names are provided for specific information; use does not constitute endorsement.

the GPS option requires reception of acceptable signals from a minimum of four satellites. Satellite shading by vegetation and topography reduced the number of radar traverses with acceptable satellite signals to the two highest-lying lines.

The GPR traverses crossed areas of Berks-Weikert shaly silt loams, 15 to 25% slopes (BID), and Berks-Weikert association, steep (BMF). The well drained, shallow Weikert and moderately deep Berks soils formed in residuum weathered from shale. Depths to paralithic bedrock range from 10 to 20 inches for Weikert and 20 to 40 inches for Berks soils. The taxonomic classifications of these soils are listed in Table 1.

The radar traverses were completed by pulling the 400 MHz antenna through the woods. In general, traverses lines were orientated parallel with slope contours. Each radar traverse was stored as a separate file. Using the *Interactive Interpretation* module of the RADAN processing software, depths to the bedrock were quickly, automatically, and reasonably accurately picked and outputted to a file (X, Y, Z format; containing latitude, longitude, bedrock depths, and other useful data).

Permanent Grid Study:

In order to study temporal differences in the resolution, amplitudes and positioning of reflected radar signals, a permanent survey grid has been established on the lower portion of a swale within the Shale Hills Catchment. This grid is located in an area of Rushtown soils. The very deep, excessively drained Rushtown soils formed in colluvial deposits.

The dimensions of the permanent grid are 12 by 15 ft. Plastic stakes have been inserted in the ground at the four grid corners and a rope grid-lattice has been fabricated for attachment to these stakes and overlaid across the grid area. The rope lines extend across the grid (parallel with X axis) at intervals of about 13 inches and provide ground control for traverses conducted with the 400 MHz antenna. Along each rope line, distance marks are affixed at intervals of 5 feet to provide a measure of horizontal control for each radar traverse.

Two GPR surveys (October and November 2008) were completed across this grid. For each survey, traverse lines were orientated parallel to the X-axis (cross swale profiles). Following data collection along a traverse line, the 400 MHz antenna was sequentially displaced about 13 inches across the grid to the next rope line, and the process was repeated in a back-and-forth fashion. A total of 12 traverses were required to complete each GPR grid survey.

Infiltration Surveys:

The Shale Hills Catchment is underlain by fractured rock. Because of the varied distribution and connectivity of fractures, the shale offers highly complicated flow paths, which are difficult characterize. In this study, GPR and time-domain reflectometry (TDR) are being used to better understand and characterize ground-water flow paths in the soils over fractured bedrock, at scales of one to several meters.

In October, a small grid was established in an area of Weikert soil located on a south-facing, back-slope component. The dimensions of this grid are 200 by 100 cm. To complete a GPR survey, eleven, 200-cm long traverses were made across the grid with a 400 MHz antenna. The interval between successive traverses was 10 cm.

In November, the study was repeated across the Weikert grid, and a new grid was established in a swale and area of Rushtown soils. The dimensions of the Rushtown grid are 150 by 90 cm. To complete a GPR survey, ten, 150-cm long traverses were made across the Rushtown grid with a 400 MHz antenna. The interval between successive traverses was 10 cm.

At each site (Weikert and Rushtown), a shallow trench was excavated immediately up slope from the grid. For each survey and grid, two *dry* surveys were completed prior to the application of any water into this trench. At each site, the trench was then filled with water. GPR surveys were completed of each grid immediately following the application of water and at intervals of 10 minutes for twenty minutes (3 surveys). The trench was then refilled with water and the process repeated. These procedures provided eight complete GPR surveys of each of the two grids. TDR probes were inserted in trenches located immediately up slope (also used for water dumping) and down slope of the grids.

Results:

GPR/GPS Survey

The Berks and Weikert soils are considered to have moderate potential for most GPR applications. The low to moderate clay contents of these soils (ranges from 5 to 32 % for Berks, and 15 to 27 % for Weikert soils) result in moderate rates of signal attenuation. However, the large numbers of rock fragments in these soils produced unwanted scattering losses, which restrict penetration depths, obscure the soil/bedrock interface, and confounded interpretations of radar records. In addition, the large number of rock fragments in the soil weakens the dielectric contrast between the soil and the underlying shale bedrock.

On radar records collected in areas of Berks and Weikert soils, the soil/bedrock interface varied from well-expressed to obscure. The visibility of this interface on radar records is dependent on its depth and topography; the number of rock fragments and other scattering bodies (e.g., roots, burrows, disrupted or segmented layers) in the overlying soil column; differences in moisture contents, and the internal structure of the underlying bedrock. On radar records, the soil/bedrock interface was interpreted based on differences in signal amplitude, reflective patterns, and continuity. Figure 1 is a representative portion of a radar record from an area of Weikert soils. On this radar record, the interpreted soil/bedrock interface has been highlighted with a segmented, green-colored line. In general, the bedrock interface is identified by higher-amplitude (white and gray colored), more continuous, linear reflectors. On the radar record shown in Figure 1, the overlying soil materials appear to be relatively free of larger coarse fragments and high-amplitude radar reflections. Some reflections are evident in the soil, but these reflections are either of weaker signal amplitudes, discontinuous, or appear as point anomalies (interpreted to represent larger rock fragments rather than parent rock).

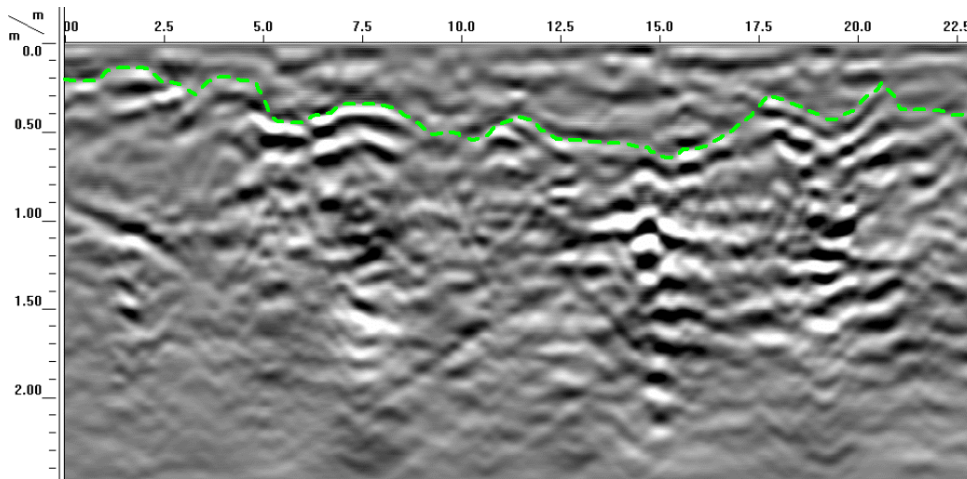


Figure 1. This 2D radar record was collected in an area of Berks-Weikert shaly silt loams, 15 to 25% slopes. The segmented green line indicates the interpreted soil/bedrock interface.

The underlying Rose Hill formation consists of thinly bedded, highly fractured, folded and faulted olive-colored shale that is intercalated with thin layers of gray siltstone and red hematitic sandstone (Folk, 1960). On most radar records from the Shale Hills Catchment, fracture and bedding planes of the Rose Hill formation were not apparent. In Figure 1, while generally absent, inclined and highly segmented interfaces of varying signal amplitudes are assumed to represent fracture and/or bedding planes. The bedrock itself contains a large number of low amplitude hyperbolic reflections and diffraction tails. These features are produced by small-scale, scattering bodies or inhomogeneities in the bedrock. The presence of a large number of hyperbolas was used as an indicator of the shale bedrock.

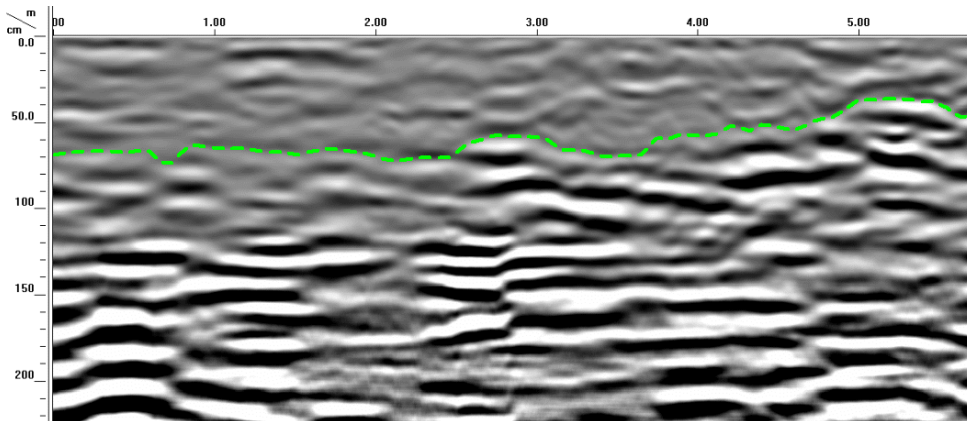


Figure 2. This 2D radar record was also collected on an area of Berks-Weikert shaly silt loams, 15 to 25% slopes. The segmented green line indicates the interpreted soil/bedrock interface.

Figure 2 is a radar record from an area of Berks soils that is underlain by bedrock having well expressed bedding and fracture planes. On this radar record, the interpreted soil/bedrock interface has been highlighted with a segmented, green-colored line. Once again, the overlying soil materials are characterized by the absence of high-amplitude radar reflections. As a general rule, on portions of radar records with well expressed bedding and fracture planes, hyperbolas are generally absent within the bedrock. However, without knowledge of location and assumptions of underlying soil depths and properties, it is difficult to distinguish planar reflections caused by bedding and fracture planes from those produced by stratigraphic layers (in swales and along the stream channel).

Laterally, the soil/bedrock interface produces reflections of varying signal amplitude. In the first 2.5 m of the radar record shown in Figure 2, the soil/bedrock interface is poorly expressed and difficult to follow with confidence (different color tables and transforms were used to clarify and draw this interface). Here, the interface is assumed to be more transitional; possibly the result of greater numbers of rock fragments in the soil, the moisture contents of the adjoining materials, and/or the more intricate and irregular topography of the bedrock surface. The interface is more clearly expressed in the last 3 m of this radar record.

Four radar traverses were conducted across the south-facing summit and back slopes of the catchment (see Figure 3). However, because of satellite shading by vegetation and topography, an acceptable level of GPS signal reception was achieved only along the two highest lying traverse lines. On the two lower-lying traverse line, poor satellite reception resulted in larger position errors and the superimposing of some radar data (longer, straighter lines connect points that have been interpolated without adequate GPS position data; this data overlaps more correctly positioned data on the two lower-lying traverses).

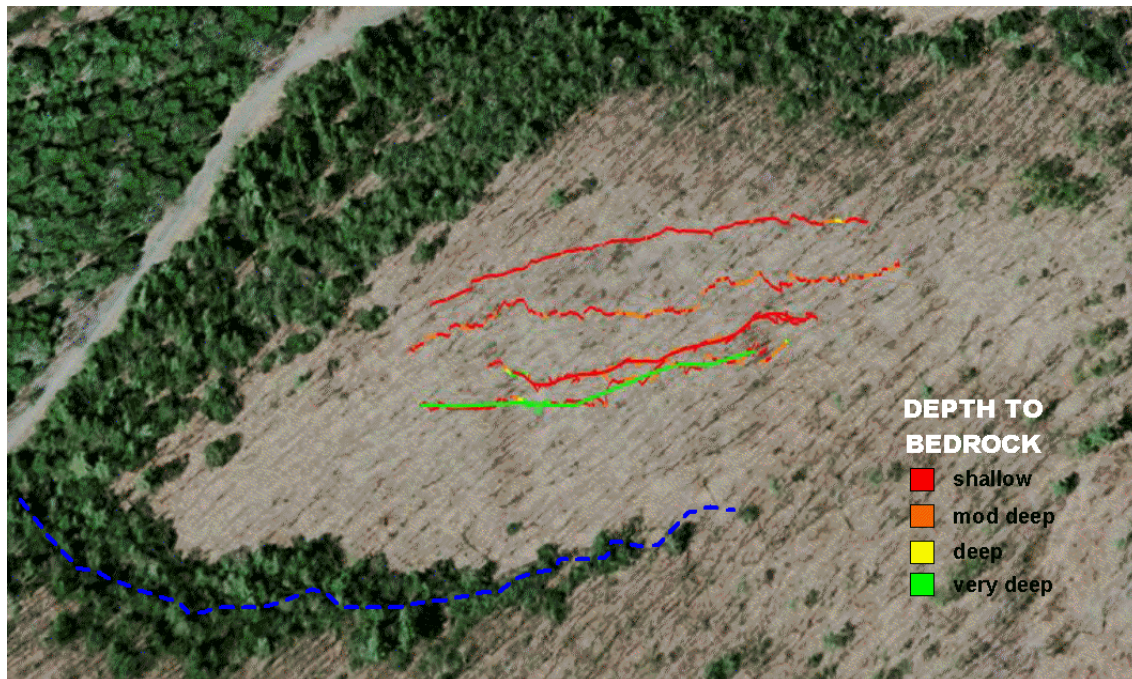


Figure 3. *The depth to bedrock as interpreted from radar records collected along the northern portion of the Shale Hills Catchment. The lower-lying (southerly) GPR traverses were noticeably impacted (overwrite; straight, highly-interpolated lines between incorrect positions) by poor satellite reception and positioning errors.*

Figure 3 is a Google Earth image showing the locations and interpreted soil depths along these traverse lines. Although the scale is small and it is difficult to see all the depth intervals, it is obvious that shallow and moderately deep soils (colored red and orange, respectively) dominate the traversed areas.

Because of positioning errors, only data from the two higher-lying traverses are reported. Along these traverse lines a total of 53307 radar scans were georeferenced. Along these two traverse lines, based on soil depth criteria, 76 % of the observations are shallow; 23 % are moderately deep, and 1 % is deep to bedrock. The average depth to bedrock is about 40 cm with a range of about 9 to 112 cm.

Tables 2 and 3 summarize the results for these two GPR traverse lines. The techniques used in these surveys are novel (GPR and GPS), and the number of observations is extraordinarily large. Table 2 provides the basic statistics for these traverses. Table 3 lists the number and frequency of observations for each traverse according to soil depth classes.

Table 2. Basic statistics for the depth to bedrock along the two most northerly radar traverse lines shown in Figure 3.

Traverse Line	1	2
Minimum	9.14	15.00
25%-tile	20.97	38.71
75%-tile	38.71	53.71
Maximum	112.36	97.25
Mean	31.63	46.77
Std deviation	15.82	15.86

Table 3. The number and frequency distribution of observations (by soil depth classes) along the two most northerly radar traverse lines shown in Figure 3.

Traverse Line	1	2	1	2
	<i>Number</i>	<i>Number</i>	<i>Frequency</i>	<i>Frequency</i>
Shallow	21693	18865	0.94	0.63
Moderately Deep	1190	11303	0.05	0.37
Deep	256	0	0.01	0.00
Total	23190	30168	1.00	1.00

Permanent Grid Site:

Two 3D GPR pseudo-images that were constructed from data collected on the permanent grid are shown in Figure 4. In Figure 4, the left-hand and right-hand images were constructed from data obtained with a 400 MHz antenna in October and November of 2008, respectively. The soils were slightly moister in October than in November (having ϵ_r of 8.05 and 7.42, respectively). Both 3D GPR pseudo-images shown in Figure 4 were submitted to the identical processing (migration, horizontal high pass filtration, and range gain adjustment). The same display gain adjustments were used to enhance subsurface reflections. These 3D GPR pseudo-images were not terrain correction.

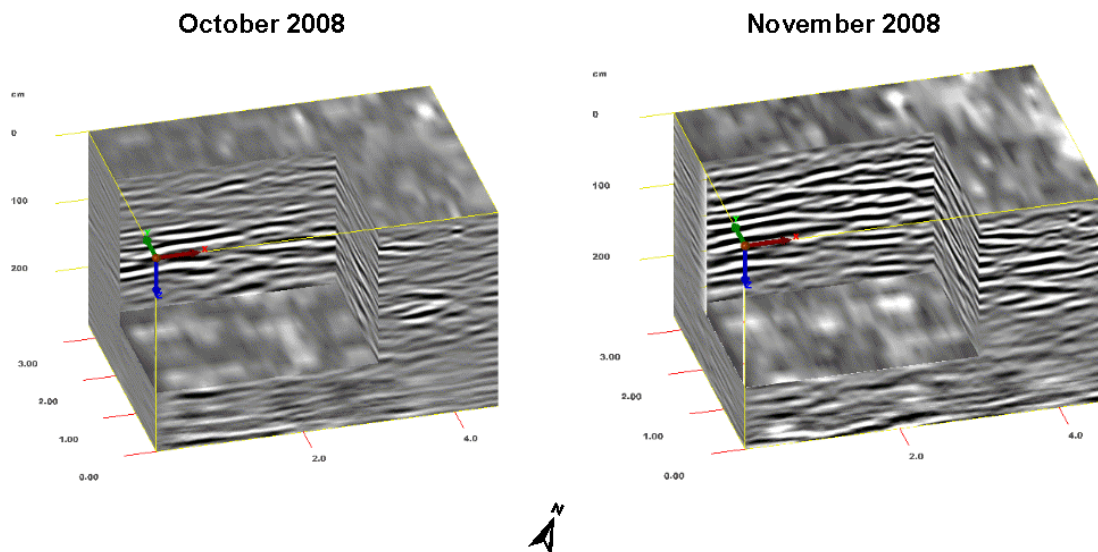


Figure 4. The radar records used to construct these two 3D pseudo-images of the permanent grid site were collected two months apart. The grid was created from GPR traverses, which were run parallel to X axis. In each image, a 3 x 2.13m x 200 cm inset cube has been graphically removed.

In both of the pseudo-images shown in Figure 4, a 3 by 2.13 by 2 m inset cube has been graphically removed to reveal the subsurface structure. In general, the data obtained on these two separate occasions are comparable and produce similar subsurface patterns. Although the same range and display gain functions were used, subsurface amplitudes are noticeably higher for the November survey. The increased amplitudes of subsurface reflections for the November survey are attributed principally to differences in gain settings on the SIR-3000 rather than differences in soil moisture contents. In general, broader break point intervals and higher gain settings were used for the November survey. For the October survey, the following signal gain values were applied to 5 gain points: -20, 5, 35, 40, and 50. For the November survey, the following signal gain values were applied to 4 gain points: -20, 20, 35, and 55. This disparity is unfortunate, but was based on subtle differences in signal strength over the calibration site. For time-lapsed data collection, additional concerns and greater attention to details are required when calibrating the GPR. It is recommended that an additional survey of the site be conducted in a moister time of the year (March) with the same gain settings and number of break points as used in the November 2008 survey.

Compared with the imagery collected in October, subsurface reflections appear noticeably stronger on the imagery collected in November. However, disregarding differences in signal amplitudes, the structure and geometry of subsurface strata are remarkably similar on the two 3D pseudo-images shown in Figure 4. On these 3D pseudo-images, a sequence of stratigraphic layers is evident within the column of colluvium that fills the swale. These 3D pseudo-images provide a means of visualizing and interpreting the 3D continuity of these layers. As radar scans were continuously collected in the direction of the radar traverse (along the X axis; right foreground), subsurface features are better resolved along this direction of radar travel. In the orthogonal direction to the radar traverse (along the Y axis), images are interpolated between successive GPR traverses. Along this axis, images are more distorted and poorly resolved (spatial aliasing), and appear smudged.

Infiltration Experiment:

These GPR surveys were conducted on two grid sites to observe differences in subsurface reflection patterns associated with the flow of water through profiles of Weikert and Rushtown soils. Figure 5 contains two radar records that were collected along the first traverse line at the Weikert grid site (October 2008) during the first and second *dry* runs. All settings are the same for each record. Although these two radar records are remarkably similar, variations in signal strengths and interface depth and continuity are evident. As these two traverses were collected within 5 minutes of each other, differences are attributed to very slight displacements in antenna positioning and variations in the antenna coupling and speed of advance along the traverse line. These differences emphasize the need for additional standards and procedures when conducting time lapsed GPR surveys.

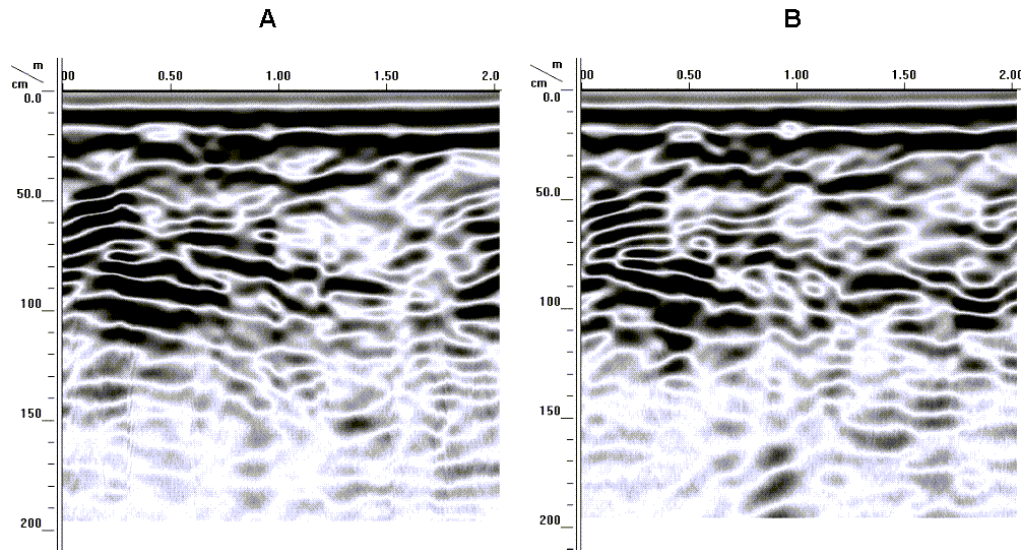


Figure 5. These two 2D radar records were collected (October 10) under dry conditions along the first line of the Weikert infiltration grid site.

Survey setup and operational procedures are inherited from my nearly thirty years of GPR field work. The use of 3D and 4D (time lapsed) GPR is novel and our work at Shale Hill has brought attention to the additional procedural concerns. The 400 MHz antenna was operated in the time mode without the aid of a survey wheel. When operated in the time mode, the number of scans per unit

distance is dependent on the scanning rate (set on SIR-3000) and the speed of advance, which did vary along and among each traverse line (different file sizes). Although the distance between each 50-cm marker along a GPR traverse line was *normalized* during data post-processing, the number of scans per interval did vary and influenced the amplitudes and phase information displayed on the 2D and 3D radar images. It was also observed that the antenna did not remain completely coupled to the ground surface during surveying. A very slight, but varying tilt in the antenna was observed during grid work. This tilt would influence the antenna's coupling with the soil, which would introduce inconsistencies in reflected signal amplitudes. Finally, the rope mesh used to guide the antenna is flexible, which will allow slight spatial discrepancies in antenna positioning as it pressed or wandered from the ropes during each traverse. These potential sources of error were discussed with some of the GSSI staff (Roger Roberts, David Cist, Dan Delea, and Brian Jones) during a conference on 10 December 2008. During this conference, radar records from the grid site were reviewed. The representatives from GSSI suggested that a survey wheel or cart and a more rigid grid frame (suggested wooden frame) be used in these surveys to help reduce these sources of errors.

In any time-lapsed infiltration experiment, it is only natural to attribute differences in signal amplitudes and spatial patterns to variations in the distribution of soil moisture over time. The radar records shown in Figure 5 suggest that such an interpretation, under field conditions, could be hazardous. These results suggest that radar interpretations should be advanced with both caution and trepidation.

Figure 6 contains six time-lapsed, 2D radar records of the first traverse line (one nearest the infiltration trench) for the October 2008 survey of the Weikert grid. The trench was filled with water just prior to the 16:35 and 17:15 surveys. In general, the amplitude of reflected signals appears stronger immediately after the trench was filled with water (the 16:35 and 17:15 2D records). Radar records collected at later times show an apparent drop in signal amplitudes and a slight delay in two-way travel times to some interfaces. These characteristics are believed to represent effects of the redistribution and flow of ground water. However, both surface and subsurface signal amplitudes for the 16:55 survey appear more intense and are therefore considered inconsistent. As the settings on the SIR-3000 were not adjusted, staff at GSSI suggested that the observed discrepancy may reflect differences in survey speed and/or antenna tilt. A slower speed of advance and less antenna tilt could produce more intense reflections.

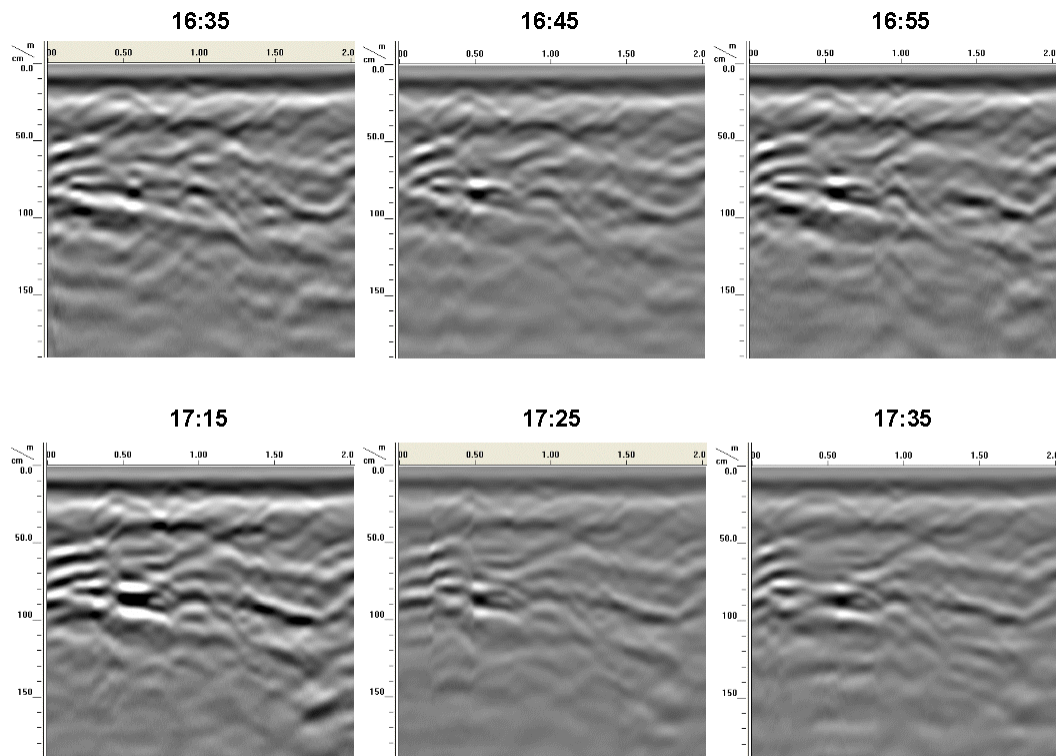


Figure 6. These 2D radar records show the affects of infiltrating water on the grid line that was nearest to the discharge trough at different times (October survey).

It is difficult to show the effects of water infiltration in solid 3D cube images. Figure 7 contains two columns of three, 3D transparency pseudo-images of the Rushtown grid. Each column of 3D transparency images shows radar data collected under dry

conditions (upper), immediately after initial watering (middle), and after 1 hr following watering. In Figure 7, the left-hand column contains GPR transparency images that were minimally processed (setting the initial pulse to time zero, color table and transformation selection, display range gain adjustments); data used for the right-hand column were subjected to the same processing procedures plus migration (constant velocity) and finite impulse response filtration (FIR). A FIR filter was used because it provides a finite duration impulse response, which is symmetrical and has linear phase characteristics. These characteristics of the FIR filter result in no significant shifts in either time or phase. All 3D pseudo-images are 45 % transparency with a resolution of 1:8.

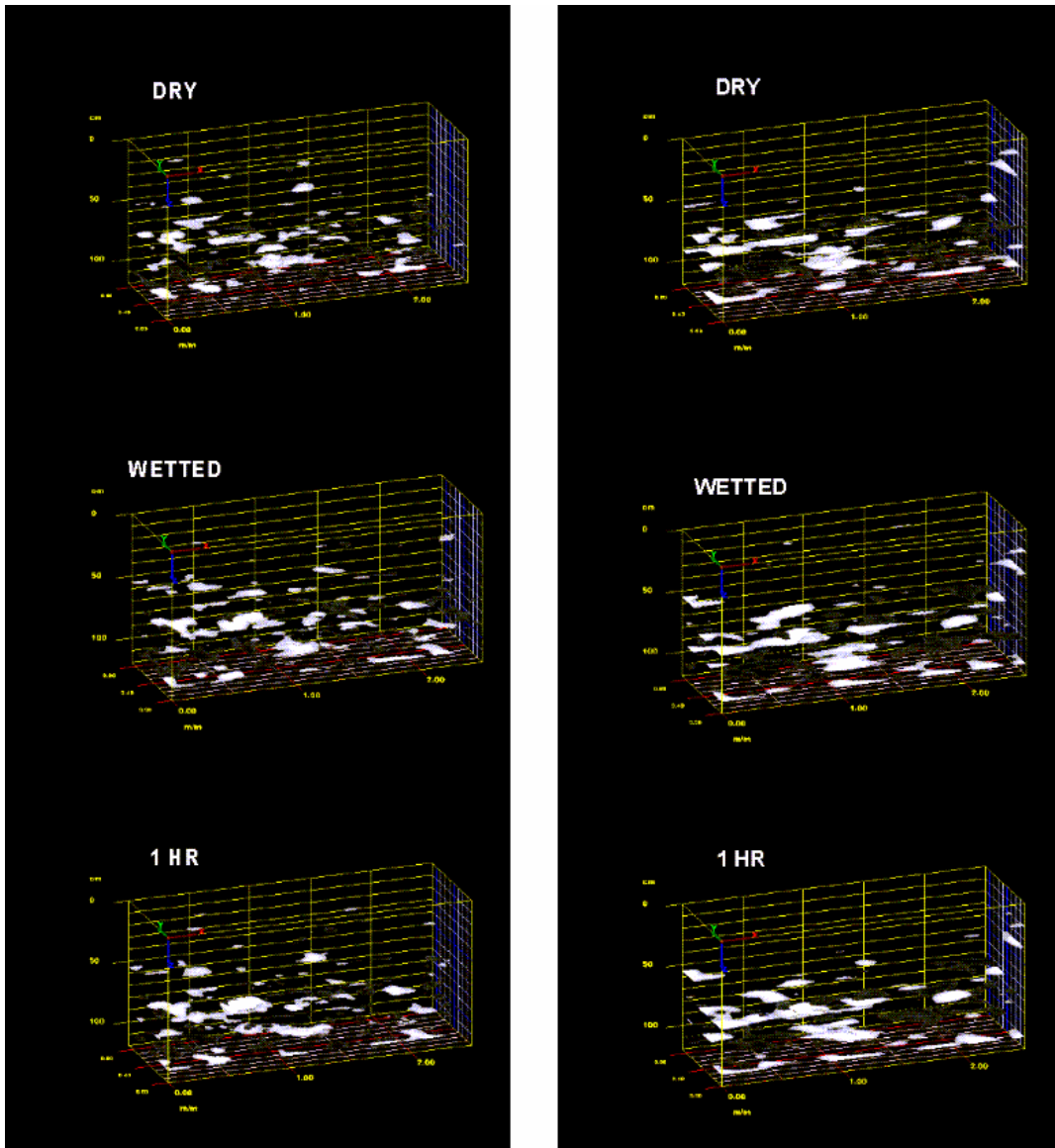


Figure 7. These 3D transparency pseudo-images are from the Rushtown grid. Pseudo-images in the left-hand column show data that have been minimally processed. Pseudo-images in the right-hand column show data that have been subjected to migration and high-pass finite impulse response filtration (FIR). Each column shows radar phase data collected under dry conditions (upper), immediately after initial watering (middle), and after 1 hr following watering.

In Figure 7, the most apparent differences in the transparencies can be attributed to differences in the type and amount of applied processing. The imagery is more similar within than between the two columns. Migration (images on right) has resulted in seemingly larger and more horizontally continuous, high-amplitude, planar reflections. With the exception of these more noticeable differences caused by processing, only some very slight, minor, and seemingly random changes to spatial patterns are evident in these time-lapsed images. No noticeable and/or structured changes in spatial patterns, which can be associated with the flow of water, are evident in these pseudo-images. This matter was also discussed with the staff at GSSI. For the detection of very small-scale and subtle

differences in the soil properties, they suggest conducting more closely spaced, better controlled radar traverse with a survey wheel. Through their discussions with Mark Grasmueck of the University of Miami, they recommend the use of higher frequency antennas and traverse intervals of 2.5 cm to resolve such small scale features. However, they provided no assurance that these measures would work and show infiltration patterns in the soils at Shale Hills.

Both Dean Goodman of GPR-Slice and David Cist of GSSI suggested the use of Hilbert Transformation to improve ground-water flow pattern recognition on 3D GPR transparency pseudo-images. Following standard and minimal processing, data collected at the Rushtown grid, was transformed. The 3D GPR transparency pseudo-images shown in Figure 7 have been processed using the Hilbert Transformation. In these 3D pseudo-images the magnitude (rather than the phase) of the reflected signals are shown. Each image was similarly processed and displayed with a 25 % transparency and a resolution of 1:128. The Hilbert Transform uses magnitude to decompose or compact hyperbolic reflectors and multiple "echoes" (Oppenheim and Schafer, 1975). This technique reduces clutter and can be used to help resolve subsurface features. As evident in Figure 7, the use of the Hilbert Transform, did improve the definition of high-amplitude, subsurface reflectors. As most of these reflectors appear at deeper soil depths (>100 cm) and are planar, they are believed to represent major bedding planes in the underlying shale. Though slight, the most noticeable time-lapsed difference in the shape and distribution of these patterns are evident immediately following the application of water into the upslope trench (compare *DRY* with 1505 pseudo-images). However, without additional imaging processing software, which can be used to quantify these apparent differences, only qualitative descriptions of changes in amplitudes and spatial patterns are possible.

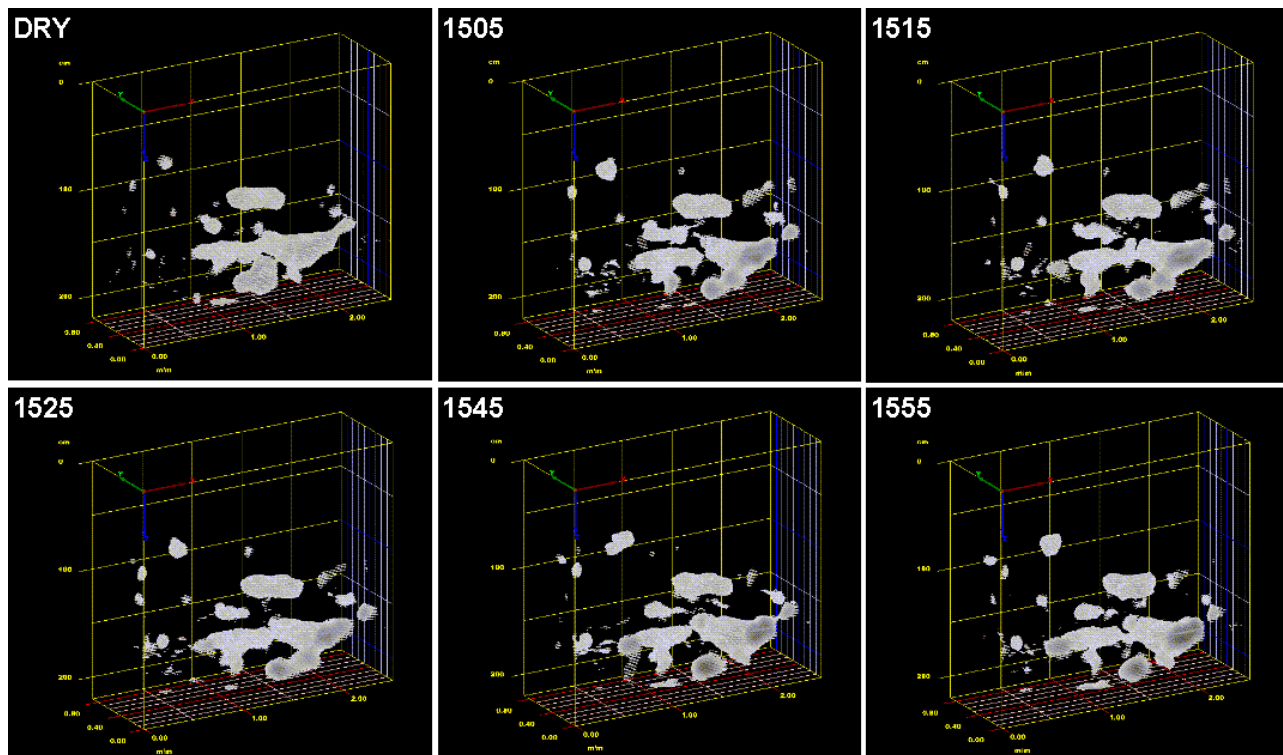


Figure 8. These 3D transparency pseudo-images from the Rushtown site have been minimally processed, except being subjected to Hilbert Transformation. Pseudo-images show radar amplitude data collected under dry conditions, immediately after initial and secondary watering (upper and lower middle, respectively), and after 10-minute time intervals (1515, 1525, 1555) following watering.

EMI Survey of Klepler Farm:

Survey Procedures:

A mobile EMI surveys was completed at Klepler Farm. The EM38DD meter was operated in the continuous mode with measurements recorded at a ½ sec interval. The meter was placed in a plastic sled with its long axis orientated parallel to the direction of travel and towed behind an ATV at speeds of 1 to 3 m/sec. The EMI survey of Klepler Farm was completed by driving the ATV at a uniform pace along rows of stubble, in a random or back and forth manner. In fields that were not harvested, a pedestrian survey was completed with the EM38DD carried about 2.5 to 5 cm above the ground surface along rows (corn).

Results:

Table 1 summarizes the results of the EMI survey that was completed on the research fields at Klepler Farm. The EC_a data were not temperature corrected. The relatively low EC_a recorded across these fields reflect the electrically resistive nature of soils and underlying limestone bedrock. For the shallower-sensing (0 to 75 cm) horizontal dipole orientation (HDO), EC_a ranged from -4.8 to 368.0 mS/m. The large range in EC_a values reflects the presence of buried utility lines and artifacts within portions of the fields. In the HDO, EC_a averaged 12.9 mS/m with a standard deviation of 7.8 mS/m. However, a large number (one-half) of the EC_a measurements recorded in the HDO were between about 11.0 and 14.5 mS/m. For the deeper-sensing (0 to 150 cm) vertical dipole orientation (VDO), EC_a ranged from -125.0 to 194.0 mS/m. Once again, the large range in EC_a reflects the presence of buried artifacts. In the VDO, EC_a averaged 13.6 mS/m with a standard deviation of 4.6 mS/m. One-half the EC_a measurements recorded in the VDO were between about 11.4 and 15.6 mS/m.

Table 1
Basic EMI Statistics for the EMI survey that was conducted at the Klepler Farm Research Site on 12 November 2008.
(Other than the number of observations, all values are expressed in mS/m)

	HDO	VDO
Number	18740	18740
Minimum	-4.75	-125.00
25%-tile	11.00	11.38
75%-tile	14.50	15.63
Maximum	368.50	194.50
Average	12.93	13.61
Standard. Deviation	7.81	4.56

The large range in recorded EC_a reflects the presence of buried utility lines within portions of the fields. Buried power cables entered the south-central portion of the study site along a farm road. These utilities produced electromagnetic interference resulting in anomalous EMI responses. Other anomalous EC_a measurements reflect metallic artifacts that were either discarded or shallowly-buried in the field and crossed or closely approached with the meter during the survey.

Figure 9 contains two, two-dimensional plots of the EC_a data that were measured with the EM38DD meter in the horizontal (upper plots) and vertical (lower plots) dipole orientations. In each plot, the isoline interval is 4 mS/m and the same color ramp is used. Spatial EC_a patterns appearing in Figure 9 are assumed to be principally related to differences in soil depth and wetness. Areas with lower EC_a are on higher-lying, more sloping, better drained landscape components. In general, these areas have thinner caps of residuum and shallower depths to limestone bedrock. Areas with higher EC_a are on lower-lying, more imperfectly drained plane and concave slope components. In general, these areas are wetter, and have thicker caps of residuum and deeper depths to bedrock.

In the plots shown in Figure 9, the approximate locations of buried utility lines can be identified by anomalous EC_a values plotted in the extreme south central portion (most evident in the upper plots) of the research fields. The northern portion of the research site also contains buried utility lines, but this area was avoided.

The spatial EC_a patterns evident in the plots of Figure 9, are closely similar to those obtained during previous EMI surveys that were conducted this year. These spatial similarities suggest the presence of spatially stable hydrogeologic functional units as defined with EMI.

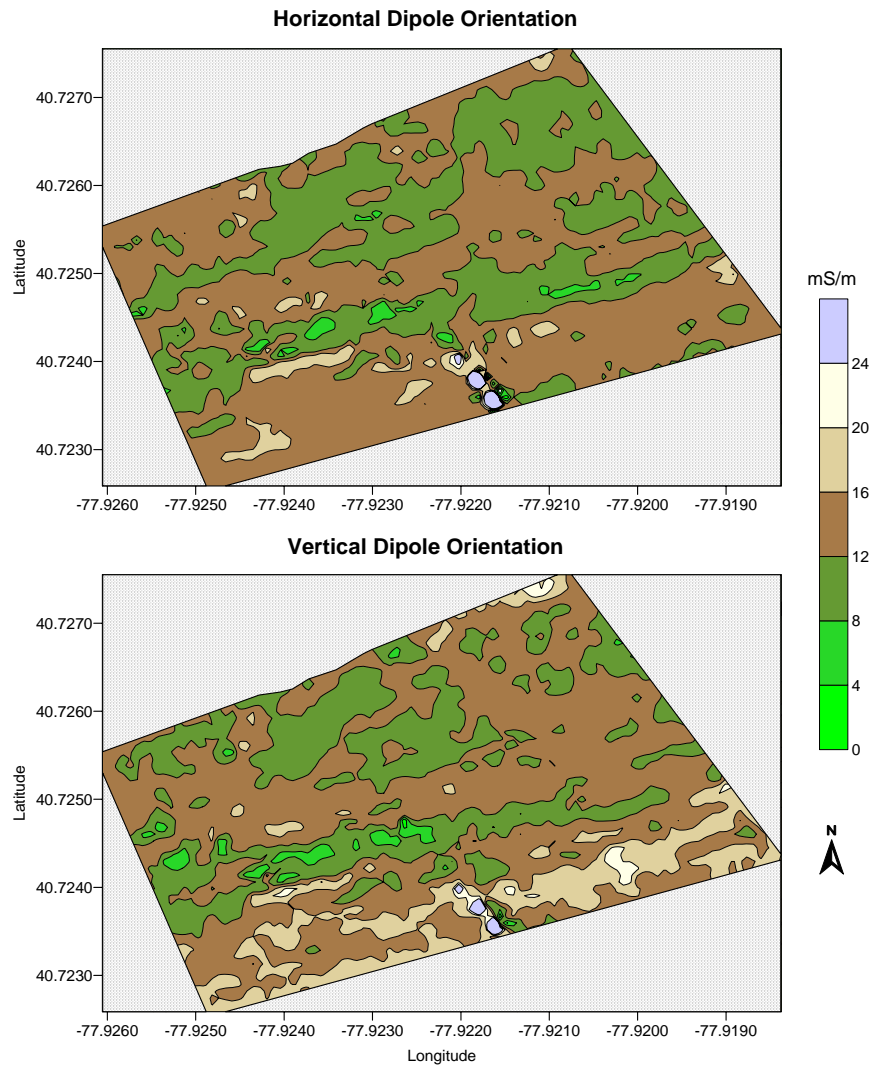


Figure 9. Plots of EC_a data collected in the shallower-sensing horizontal (upper) and deeper-sensing vertical (lower) dipole orientation at Klepler Farm.

References:

- Conyers, L. B., 2004. Moisture and soil differences as related to spatial accuracy of GPR amplitude maps at two archaeological sites. 435-438 pp. IN: Proceedings of the 10th International Conference on Ground Penetrating Radar. 21 to 24 June 2004, Delft, The Netherlands.
- Daniels, D. J., 2004. Ground Penetrating Radar; 2nd Edition. The Institute of Electrical Engineers, London, United Kingdom.
- Folk, R. L., 1960. Petrography and origin of the Tuscarora, Rose Hill, and Keefer formations, Lower and Middle Silurian of eastern West Virginia. *Journal of Sedimentary Research*; 30 (1): 1-58.
- Geonics Limited, 2000. EM38DD ground conductivity meter: Dual dipole version operating manual. Geonics Ltd., Mississauga, Ontario.
- Oppenheim, A. V., and R. W. Schaffer, 1975. Digital Signal Processing. Prentice Hall, Inc. Englewood Cliffs, NJ.
- Robinson, D. A., A. Binley, N. Crook, F. D. Day-Lewis, T. P. A. Ferré, V. J. S. Grauch, R. Knight, M. Knoll, V. Lakshmi, R. Miller, J. Nyquist, L. Pellerin, K. Singha, and L. Slater., 2008. Advancing process-based watershed hydrological research using near-surface geophysics: a vision for, and review of, electrical and magnetic methods. *Hydrological Processes* 22: 3604-3635.